14. Hanley, H. J. M., and M. Klein, *NBS Tech. Note 360* (1967).
15. Hill, T. H., "An Introduction to Statistical Thermodynamics," Addison-Wesley, Reading, Mass. (1960).
16. Hirschfelder, J. O., C. F. Curtiss, and R. B. Bird, "Molecular Theory of Gases and Liquids," Corrected Printing with Notes Added, Wiley, New York (1954).
17. Keller, J. B., and B. Zumino, *J. Chem. Phys.*, **30**, 1351 (1959).
18. Klein, M., *J. Res. NBS*, **70A** (3), 259 (1966).
19. Kobe, K. A., and R. E. Lynn, Jr., *Chem. Rev.*, **52**, 117 (1953).
20. Kretschmer, C. B., and R. Wiebe, *J. Am. Chem. Soc.*, **76**, 2579 (1954).
21. Kunz, R. G., Ph.D. thesis, Rensselaer Polytechnic Inst., Troy, N. Y. (1968). University Microfilms, No. 69-2466, Ann Arbor, Mich.
22. ———, and R. S. Kapner, *J. Chem. Eng. Data*, **14**, 190 (1969).
23. Lambert, J. D., G. A. H. Roberts, J. S. Rowlinson, and V. J. Wilkinson, *Proc. Roy. Soc. (London)*, **A196**, 113 (1949).
24. Lennard-Jones, J. E., *ibid.*, **A106**, 463 (1924).
25. MacCormack, K. E., and W. E. Schneider, *J. Chem. Phys.*, **19**, 849 (1951).
26. Masia, A. P., M. D. Pena, and A. B. Lluna, *Anal. Real Soc. Espan. Fis. Quim. (Madrid)*, **B60**, 229 (1964).
27. Moreland, M. P., J. J. McKetta, and I. H. Silberberg, *J. Chem. Eng. Data*, **12**, 329 (1967).
28. Newton, R. H., *Ind. Eng. Chem.*, **27**, 302 (1935).
29. O'Connell. J. P., and J. M. Prausnitz, *Ind. Eng. Chem. Process Design Develop.*, **6**, 245 (1967).
30. Pauling, L., "The Nature of the Chemical Bond," 3rd edit., Cornell Univ. Press, Ithaca, N. Y. (1960).
31. Robinson, J. D., Ph.D. thesis, Univ. Delaware, Newark (1968).
32. Rowlinson, J. S., *Ind. Eng. Chem.*, **59** (12), 28 (1967).
33. ———, *Bull. 201 Eng. Exp. Sta. Ohio State Univ.*, Columbus (1967).
34. Tee, L. S., S. Gotoh, and W. E. Stewart, *Ind. Eng. Chem. Fundamentals*, **5**, 356 (1966).
35. Weast, R. C., "Handbook of Chemistry and Physics," 47th edit., Chemical Rubber Co., Cleveland, Ohio (1966).

Manuscript received November 4, 1969; revision received March 11, 1970; paper accepted March 16, 1970. Paper presented at AIChE Atlanta meeting.

Heat and Mass Transfer in the Vicinity of the Triple Interline of a Meniscus

P. C. WAYNER, JR. and C. L. COCCIO

Rensselaer Polytechnic Institute, Troy, New York

Effective experimental and theoretical techniques for studying the heat transfer characteristics of a stationary evaporating meniscus formed on a flat plate immersed in a pool of liquid were developed. Integral heat transfer data were obtained for the four systems: 304 stainless steel-water, 6061 aluminum-water, 304 stainless steel-methanol, and 6061 aluminum-methanol. High rates of heat transfer were obtained in the triple interline region with a stable meniscus. Detailed descriptions of the heat flux and temperature field were obtained for the stainless steel-water and stainless steel-methanol systems. The effect of the evaporation coefficient on the heat flux distribution was evaluated. The heat transfer process in the interline region proved to be more efficient than a simple conduction process in an evaporating liquid meniscus.

In engineering processes it is desirable to find ways of improving performance by increasing the effectiveness of the underlying phenomena. In some cases a large increase in performance can be achieved by utilizing previously neglected factors. In this vein, it is believed that the rates of heat and mass transfer in some applications can be greatly increased by the proper utilization of surface phenomena. In porous medium heat exchangers (for example, sweat cooled walls, vapor chamber fins, and suction nucleate boiling devices), a large area is covered by a thin evaporating liquid film which can be in the form of many menisci located at the exit of the capillaries, where the effects of surface phenomena are sig-

C. L. Coccio is with the General Electric Company, Schenectady, New York.

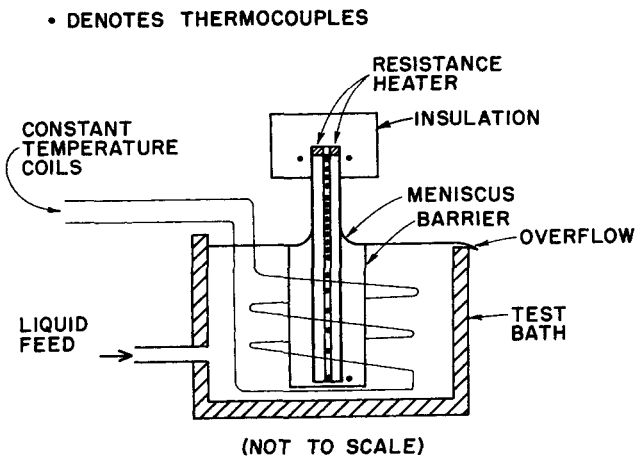

Fig. 1. Schematic diagram of heat transfer cell.

nificant. It is likely that the study of heat transfer in a stationary meniscus will prove useful in understanding and improving the performance of the porous medium heat transfer process. In addition, studies of this type will increase the understanding of related phase change processes like boiling and the flow of evaporating liquid films over heated surfaces. This paper concerns the initial study of heat and mass transfer in the vicinity of a stationary solid-liquid-vapor interline formed on a flat plate immersed in a pool of liquid. Although there have been no directly related previous studies of heat transfer in a stationary evaporating meniscus formed on a flat plate, the work evolved historically from studies of film and nucleate boiling on porous surfaces (*1* to *3*), for which it is necessary to know the heat sink capability of an evaporating meniscus. Recently, Bressler and Wyatt (*4*) evaluated the average heat flux in an evaporating meniscus formed in a capillary groove. There have been numerous studies in boiling that are indirectly related and lead logically to the work presented below.

The overall experimental approach to studying heat transfer in the meniscus consists of obtaining integral data from a pair of flat plates joined back to back and partially immersed in a pool of liquid at a controlled temperature. The free end of the plates are heated, and heat is conducted down the plates into the meniscus region. A row of thermocouples is sandwiched between the plates and provides the temperature distribution along the ensemble center line. The temperature distribution is used to obtain the heat flow rate in the plate as a function of distance from the heat source, thereby providing knowledge of the total amount of heat leaving the meniscus region. Detailed information concerning the meniscus heat transfer process is then obtained analytically from the integral data by constructing a model for the detailed temperature distribution at the solid-liquid and solid-vapor interface. The appropriateness of the model is evaluated by using the detailed temperature distribution to calculate the measured center line temperature distribution, the integral heat flow, and a portion of the liquid film profile.

EXPERIMENTAL STUDIES

Description of Equipment

A schematic drawing (not to scale) of the apparatus used to obtain integral experimental heat transfer data is presented in Figure 1. Two identical flat plates were cojoined together using RTV-108 silicone rubber cement and immersed in a pool of liquid. Before joining, the plates were machined to a tolerance of ± 0.001 in. and the surfaces were polished to a mirror finish using Linde A polishing powder on a flat wheel. The dimensions of the 301 stainless steel test plate were $3.992 \times 1.940 \times 0.112$ in. and those of the 6061 aluminum test plate were $4.000 \times 2.000 \times 0.125$ in. Calibrated 10 mil iron-constantan thermocouples were used in conjunction with a Leeds and Northrup K-4 potentiometer and a Model 9834 electronic d.c. null detector to measure the temperature distribution at the center line on the back of the plates. The thermocouples were joined to one of the plates, and the plates were separated by approximately the diameter of the thermocouple wires. The thermocouple wires ran horizontally between the plates, and the space between the wires was filled with silicone rubber cement. In the meniscus region the thermocouples were separated by a distance of 0.1 ± 0.001 in., and by a larger distance in the less sensitive regions. A total of 17 thermocouples was used. The calibration of the thermocouples was accurate to $\pm$ 0.18°F. Although there was an experimental error due to the diameter of the thermocouple bead, the size of the error was reduced by properly fitting a smooth curve to the back profile. This plate configuration resulted in a zero horizontal heat flux at the center line and a surface free from instrumentation. Electric resistance heaters were cemented to the top of the plates and connected to a d.c. power source. The heater current was obtained by measuring the voltage drop across a precision resistor. The relative error in the measurement of the power input to the heaters was less than 1%. The tops of the plates were insulated to minimize heat loss to the surroundings.

The test liquids used in the experiments were distilled water and 99.9% pure methanol. An overflow arrangement was used to maintain a constant position of the meniscus on the plate. This position and the height of the meniscus were measured relative to a bench mark with a cathetometer and telescope arrangement having an accuracy of ± 0.002 in. The relative location of the bench mark was known with respect to the thermocouples with an accuracy of ± 0.005 in. The temperature of the liquid pool was maintained constant by pumping Polyglycol P-400 heat transfer fluid through a series of coils located in the test bath. In order to minimize the effect on the meniscus of nucleation and convection from the heating coils, a barrier separated the fluid in contact with the coils from the fluid in contact with the plate. The system was open to the laboratory atmosphere during operation. Additional material concerning the experimental design was recorded in reference 5.

Operating Procedure

The steady state operation of the equipment was extremely simple. The height of the base of the meniscus was kept constant by providing a slight overflow from the test bath, while the temperature of the test bath was kept constant to $\pm$ 0.1°F. by use of a thermoregulator set to the desired bath temperature. As indicated by the reported data (T_B), the bath temperature was maintained to within several degrees of the saturation temperature. In addition, since the heat of vaporization was large compared to the heat capacity of the fluid, small fluctuations in the bath temperature had a negligible effect on the experiment. At the start of a run, it was possible to set approximately the desired plate power input. When the system reached equilibrium with the approximate settings, the thermocouple readings on the top of the plates were used to make minor adjustments in the current input in order to obtain a horizontally uniform top temperature. Steady state data could be recorded about half an hour after the final adjustment. The data recorded during a run consisted of (1) the temperature in millivolts at the center line thermocouple locations, (2) the power input to the plate heaters, (3) the positions of the top and bottom of the meniscus with respect to a bench mark on the plate, (4) the test bath temperature near the base of the plate, and (5) the ambient barometric pressure and temperature. The major difficulty encountered was fluctuations due to extraneous nucleation. While obtaining the data reported in this paper, no pulsating nucleation sites were present in the meniscus. With water a few small quiescent bubbles were attached to the metal plate in the lower part of the meniscus. With methanol extremely fine bubbles were observed coming up from the pool. In all of these tests the location of the interline appeared stable and steady to the unaided eye. Ran-

dom disturbances were undoubtedly present from nucleation sites at other locations. To the unaided eye these seemed unimportant; however, a detailed microscopic study and analysis could prove otherwise.

Experimental Results

The following solid-liquid systems were studied: 304 stainless steel-methanol, 304 stainless steel-water, 6061 aluminum-water, and 6061 aluminum-methanol. With each system tests were made with different liquid pool temperatures, and for each pool temperature tests were made at various power input levels. Data for the highest liquid pool temperatures used are presented in Figure 2. The data also represent the highest fluxes obtained without fluctuations in the meniscus due to nucleation on the barrier. However, this does not preclude the obtaining of higher fluxes with a modified experimental design.

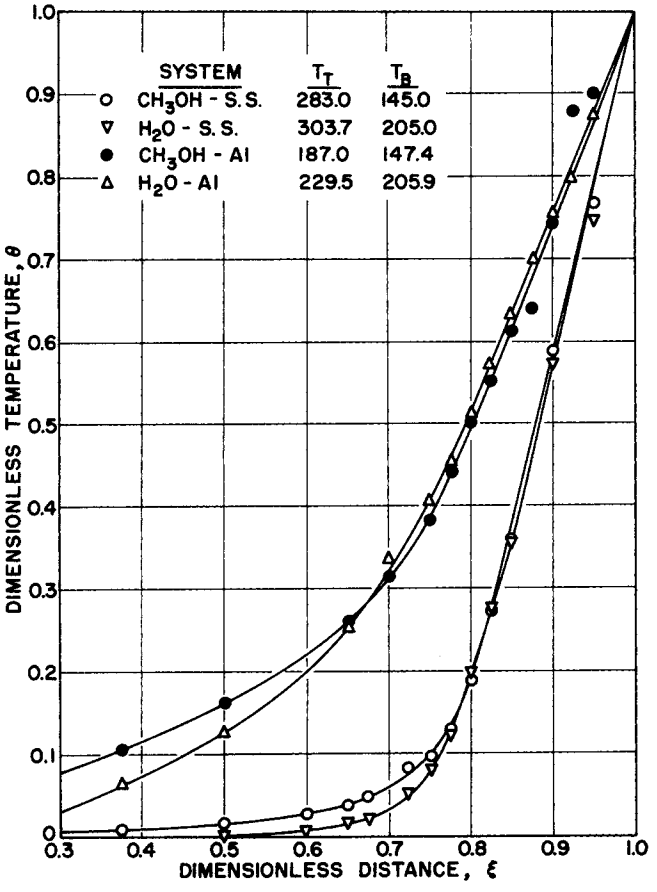

Fig. 2. Center line temperature profile.

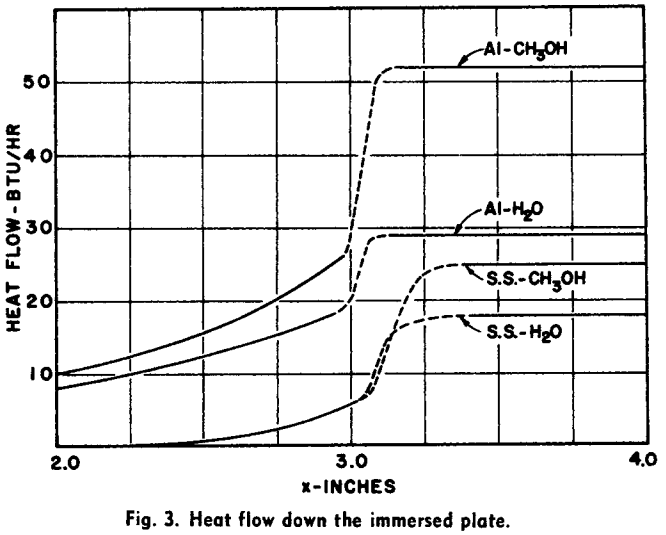

Fig. 3. Heat flow down the immersed plate.

The complete set of test data was recorded in reference 5. Except for the meniscus region, the center line temperature gradient was taken to represent the average plate temperature gradient and used to calculate the flow of heat in the plate. Later analysis demonstrated that this was a good approximation. In Figure 3 the resulting curves for heat flow versus distance are presented with the dashed sections representing the uncertain meniscus region. The results demonstrated that a relatively large heat flow out of the plate occurred over a short distance in the meniscus region. The approximate value of this heat loss can be determined from the figure.

At the start of a test run, before heating the plate, the measured equilibrium height for methanol varied between 0.0865 and 0.0949 in. This agreed with an equilibrium value of 0.091 in. for a zero contact angle calculated using Equation (*1*), which is available in the literature (*6*).

$$X = \left[\frac{(1 - \sin\phi)2\gamma}{\rho g}\right]^{1/2} \tag{1}$$

In addition, the spacing of interference fringes obtained by directing polarized monochromatic light obliquely on the plate indicated that the contact angle was approximately zero. However, due to the complexity of interfacial region, it should be indicated that the exact nature of the interline cannot be determined in this simple experimental design. During the reported tests, the measured heights for methanol were 0.0827 in. on aluminum and 0.0708 in. on stainless steel.

With water the data were less consistent. At the start of the runs reported, the equilibrium contact angle between water and stainless steel was approximately 41 deg. (0.081 in.), and approximately 20 deg. (0.113 in.) between water and aluminum. These varied from day to day in an erratic manner probably as a result of various adsorbed contaminants from the atmosphere. During the tests the meniscus heights were 0.0984 in. on aluminum and 0.0748 in. on stainless steel. Quantitatively, only the interline position is required for the analysis presented below. Qualitatively, these results demonstrated that the interline migrated down the plate so that the profile could accommodate the increased pressure gradient needed to balance the effects of viscous stress. Assuming that the contact angle remained constant, the average curvature of this meniscus was larger.

ANALYTICAL STUDIES

The usefulness of the experimental results was extended considerably through the formulation of a boundary-value problem for heat transfer in the solid plate. The two-dimensional differential equation for the steady state temperature in the plate with a constant thermal conductivity was

$$\frac{\partial^2\theta}{\partial\xi^2} + \frac{\partial^2\theta}{\partial\eta^2} = 0 \qquad \begin{matrix} 0 < \xi < 1 \\ 0 < \eta < \dfrac{b}{L} \end{matrix} \tag{2}$$

where

$$\theta(\xi,\eta) = \frac{T(x,y) - T_B}{T_T - T_B}, \quad \xi = \frac{x}{L} \text{ and } \eta = \frac{y}{L}$$

The temperature variation in the horizontal z direction was neglected because the sides of the plates were insulated and the ratio of thickness to width was small. Equation (2) was readily solved using the following boundary conditions appropriate to the experimental design,

B.C. 1 $\theta(0,\eta) = 0$ (Bottom of plate) (3)

B.C. 2 $\theta(1,\eta) = 1$ (Top of plate) (4)

B.C. 3 $\left.\dfrac{\partial\theta}{\partial\eta}\right|_{\eta=0} = 0$ (Center line) (5)

B.C. 4 (assumed) $\theta\left(\xi, \frac{b}{L}\right) = \theta_s\left(\xi, \frac{b}{L}\right)$

(Exterior) (6)

Experimental data $\theta(\xi, 0) = \theta_c(\xi, 0)$

(Center line) (7)

Boundary conditions (1) and (2) were experimentally determined. Due to the symmetry achieved with two cojoined plates, the surface at $\eta = 0$ was adiabatic. The fourth boundary condition was assumed by using a model for the temperature distribution at the plate surface. The appropriateness of the assumed profile was partially checked by using the solution to calculate the temperature profile at $\eta = 0$. Various profiles were assumed until the calculated and measured profiles at $\eta = 0$ agreed.

The required Sturm-Liouville form of the problem was obtained by making the substitution $v(\xi, \eta) = \theta(\xi, \eta) - \xi$. The problem was then solved using separation of variables, and the resulting equation for the dimensionless temperature field was found to be

$$\theta(\xi, \eta) = \xi + \sum_{n=1}^{\infty} \frac{2\cosh(n\pi\eta)\sin(n\pi\xi)}{\cosh(n\pi b/L)} \int_0^1 \left[\theta_s\left(\xi, \frac{b}{L}\right) - \xi\right] \sin(n\pi\xi)\, d\xi \quad (8)$$

Due to limitations in the accuracy of measuring and calculating the temperature profile at $\eta = 0$, there were various front profiles that could have satisfied the boundary conditions of the problem. However, physical reasoning was used to limit the choice. In the very thin film portion of the meniscus near the triple interline, heat transfer through the liquid film occurred primarily by conduction:

$$q(x) = -k_l \frac{T_s(x) - T_l(x)}{\delta(x)} \quad (9)$$

Since the film thickness vanished at the triple interline, the surface temperature of the plate at this line was equal to the surface temperature of the evaporating thin film. Although there were various interfacial effects (for example, liquid-solid interaction, thermal resistance at liquid-vapor interface) that could have increased the interline temperature above the equilibrium saturation temperature, these effects were neglected initially and the interline temperature was assumed to be the equilibrium saturation temperature. The effect of a very low evaporation coefficient was also evaluated, and is discussed below. Due to the uniform heat transfer process, the surface temperature profiles above and below the interline were assumed to be smooth functions of position. In addition the heat flux was positive and monotonically decreased both above and below the interline.

Using the above described model, the analyses of the data for two of the curves presented in Figure 2 were completed. The analyses required a lengthy iteration process and a great deal of computer time to obtain a front profile that satisfied the measured center line profile and the postulates of the model. An enlarged view of the resulting front and center line profiles in the meniscus region for the stainless steel studies is presented in Figures 4 and 5. The front profile was assumed to be a series of 27 linear segments with smaller segments used in the

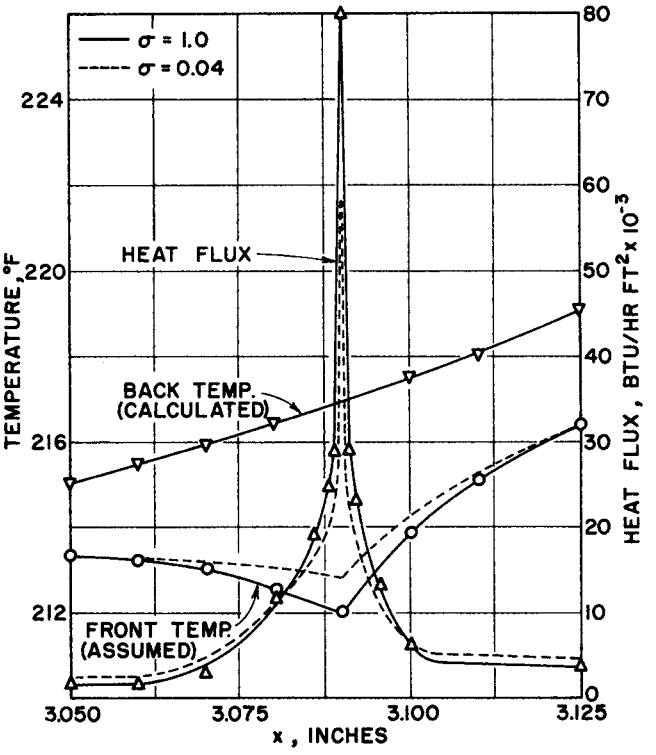

Fig. 4. Heat flux and temperature profiles; stainless steel and water.

critical meniscus region. In these figures the heat flux distribution at the surface of the plate calculated using Equation (10) with $(b - y) = 10^{-6}$ ft. is also presented.

$$q_s(x) = -\lim_{b \to y} k \left[\frac{T(x, b) - T(x, y)}{b - y}\right] \quad (10)$$

Due to the small dimension $y - b$, a considerable number of terms were required to ensure the convergence of the heat flux to the correct value. Since the front profile was assumed, the difference between the calculated and the assumed front profiles gave the degree of convergence. A definite trend in the heat flux was established with 10,000 terms, which was then extrapolated until an acceptable termination point. The convergence was considered acceptable when the residual terms could have increased the heat flux less than 10%.

Two methods were used to check the validity of the surface temperature model and the theoretical results based on it. First, the calculated center line temperature using the series solution was compared with the experimentally measured temperature. The agreement was considered adequate if the calculated profile was within ± 0.10°F. and/or ± 0.004 in. of the smoothed measured profile at all points. In addition, the heat flux was a maximum at the interline and decreased both above and below the interline. Second, the total heat flow calculated using the temperature model (Figures 4 and 5) was compared with the heat loss calculated using the measured back profiles (Figure 3). For methanol, the heat loss in the meniscus region (3.00 to 3.13 in.) calculated using the model was 22.5 B.t.u./hr., which was 18% more than the total heat loss presented in the dashed portion of the curve in Figure 3. With water, the heat loss in the meniscus region (3.00 to 3.125 in.) calculated using the model was 8.6 B.t.u./hr., which was 28% less than the total heat loss presented in the dashed portion of the curve. The difference between these two calculations was the result of a small residual heat flow in the region between the meniscus and 3.4 in., which resulted from the assumed temperature profile. Additional iterations to give convergence

beyond this point were not considered justified in the present study.

The meniscus profile in the interline region was also calculated. Assuming that heat flow in the liquid film was primarily by conduction in a direction perpendicular to the plate surface and that the liquid surface was at the equilibrium saturation temperature, Equation (9) was used to calculate the film thickness. The film thicknesses calculated using the results presented in Figures 4 and 5 are presented in Figure 6. For comparison, the equilibrium nonevaporating meniscus profiles for an assumed contact angle of 0 deg. with alcohol and with water are also presented. This wetting condition was easily obtained with alcohol. On the other hand it was not possible to obtain a constant contact angle or a wetting condition with water in a simple experiment. However, the zero contact angle represented the thinnest obtainable profile for water (neglecting disjoining pressure). These profiles were calculated using Equation (11) which was available in the literature (6).

$$\delta = \left(\frac{K}{2}\right) \ln\left[\frac{2K + (4K^2 - Y^2)^{1/2}}{Y}\right]^2 - (4K^2 - Y^2)^{1/2} + C \quad (11)$$

where

$$K = \left(\frac{\gamma}{\rho g}\right)^{1/2}$$

Assuming that the contact angle remained constant, the average curvature of the evaporating meniscus was larger (smaller radius) than its equilibrium value in order to accommodate the added effects of viscous shear. It can be further postulated that the largest effect occurred in the upper portion of the meniscus. As a result the calculated value of the evaporating meniscus should have been thicker than an equilibrium profile. Since the calculated profiles based on the experiments were found to be thinner than an equilibrium profile, the heat transfer process in the interline region was not attributable purely to conduction across an equilibrium meniscus and a higher flux model was required. However, the conduction model does present a good reference point for discussion.

The effect of the thermal resistance to evaporation on the heat flux distribution was also evaluated. There is considerable literature concerning both the theoretical liquid-vapor interfacial heat transfer coefficient and the evaporation coefficient. Among others, Nabavian and Bromley (7) presented the following form of the equation for the interfacial heat transfer coefficient:

$$h = 778 \left(\frac{2\sigma}{2 - \sigma}\right)\left(\frac{Mg_c}{2\pi RT}\right)^{1/2}\left(\frac{\lambda^2}{tV}\right) \quad (12)$$

The use of Equation (12) with an evaporation coefficient equal to unity gave a heat transfer coefficient for methanol equal to 1.9×10^6 B.t.u./(hr.)(sq.ft.)(F.), and 2.7×10^6 B.t.u./(hr.)(sq.ft.)(F.) for water. In these cases, the effect on the results would have been negligible. However, when the evaporation coefficient was assumed equal to 0.04 for water and 0.05 for methanol there was a significant effect. These values are representative of the lower range of reported evaporation coefficients (8). In Figures 4 to 6 the results obtained using the above described methods of calculation with low values for the evaporation coefficient are also presented. As expected the peak flux was found to be lower with a corresponding increase in flux in those regions removed from the interline. For methanol the heat loss in the meniscus region calculated using the model was 18 B.t.u./hr. For water it was 7.6 B.t.u./hr. In these cases the calculated film thicknesses were found to be thicker. However, they were thinner than the anticipated (although, still unknown) thickness of an evaporating meniscus.

DISCUSSION

For simplicity one would like to have postulated that the meniscus heat sink was an equilibrium meniscus adjusted for the effects of fluid flow in the meniscus across which heat flowed primarily by conduction. However, the results presented in Figure 6 indicated that the heat trans-

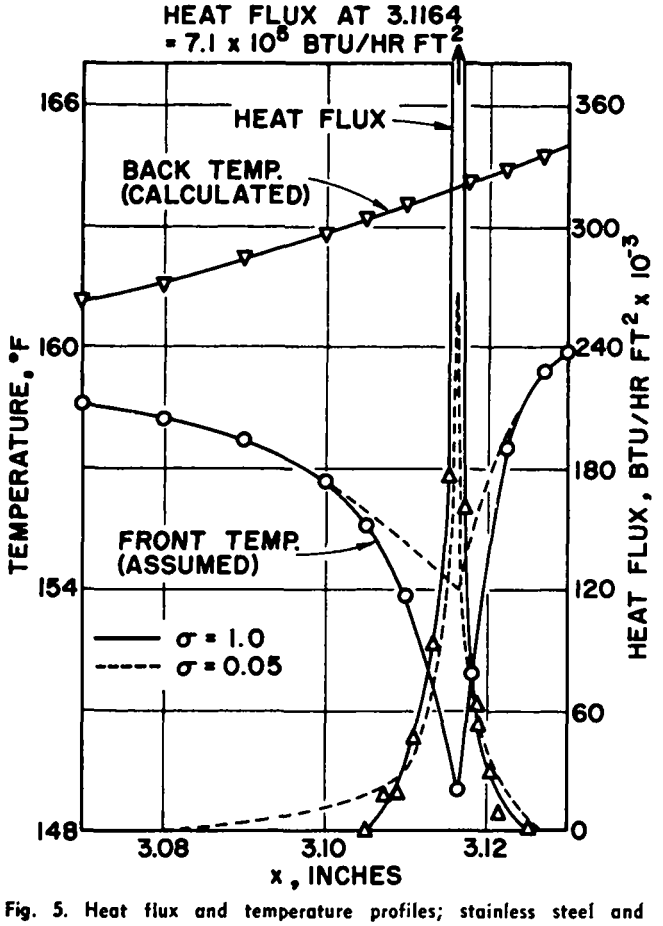

Fig. 5. Heat flux and temperature profiles; stainless steel and methanol.

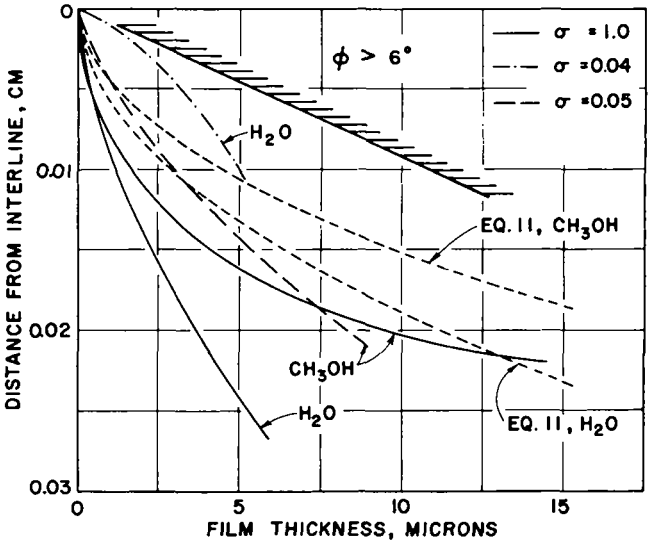

Fig. 6. Meniscus profile in the interline region.

fer process was much more complex than this simple conduction model. The main assumption that fixed the heat flux distribution was the surface temperature at the triple interline. There were two extremes in the choice of an interline temperature: an interline temperature substantially above the saturation temperature and relatively close to the center line temperature; or an interline temperature relatively close to the saturation temperature but substantially below the center line temperature. The first choice would have resulted in a relatively low uniform flux over the total meniscus region. Since it would have also required a methanol liquid-vapor interfacial temperature in the interline region approximately 11°F. above saturation (approximately 3°F. for water), it was not considered physically justified. Therefore the second limit was used with the interline temperature assumed to be saturation. Since superheat is required for nucleation, the higher temperature at the solid-liquid interface in the meniscus was acceptable. Once the interline temperature was fixed the range of profiles that fitted the data and postulates in the analysis was limited by the total heat flow. The profiles presented in Figures 4 and 5 represented one model of the heat flow. Although the relative amounts of energy leaving the various areas of the meniscus could have been slightly altered within the data and postulates, insufficient data were available to justify this effort. This was exemplified by the demonstrated effect of the controversial size of the evaporation coefficient at high rates of evaporation. However, these changes would not materially affect the basic conclusions. The integral experimental results amply demonstrated that a large heat sink was present in a stable evaporating meniscus. The temperature model indicated that it was concentrated in the interline region. Comparison of the results with a conduction model demonstrated that a higher flux model was needed to describe the heat transfer process. Various models could account for the large resultant heat flux in the interline region: for example, (1) a thin film extending above the intrinsic meniscus; (2) a sufficiently turbulent interface not detectable with the unaided eye; (3) additional convective motion due to surface tension gradients. With regard to the first model Derjaguin et al. (9), using adsorption isotherms and the disjoining pressure concept, demonstrated that thin film transport is capable of accelerating by several times the evaporation rate from capillaries. The presence of this type of flow would have had a considerable effect on the heat flux distribution. On the other hand a fluctuating or sputtering interfacial region not observable with the unaided eye could also have accounted for the large heat sink. Since there are large temperature gradients and therefore surface tension gradients, additional convective motion with upward flow in the film and downward flow along the surface could have been present. However, the relative effect of thermocapillary flow in that portion of the meniscus where the film thickness is less than 20 μ is probably small. Present studies indicate that considerable additional work is required to evaluate these various mechanisms completely.

CONCLUSIONS

1. Effective experimental and theoretical techniques for studying the heat transfer characteristics of a stationary evaporating meniscus were developed.
2. Integral heat transfer data were obtained for the four systems: 304 stainless steel-water, 6061 aluminum-water, 304 stainless steel-methanol, 6061 aluminum-methanol.
3. High rates of heat transfer were obtained in the triple interline region of a stable meniscus.
4. A detailed description of the temperature field and the heat flux was obtained for the stainless steel-methanol and the stainless steel-water systems.
5. The heat transfer process in the interline region was found to be more efficient than a simple conduction process.

ACKNOWLEDGMENT

The support of N.A.S.A. Training Grant No. 33-018-010 and N.S.F. Grant No. GK1453 entitled Suction Nucleate Boiling are gratefully acknowledged. The authors are also appreciative of the computer programming assistance given by Steven Rothman.

NOTATION

b = thickness of plate, ft.
C = constant of integration
g_c = conversion factor (ft.)(lb.$_m$)/(lb.$_f$)(sq. hr.)
g = gravitational acceleration, ft./sq.sec.
h = interfacial heat transfer coefficient, B.t.u./(hr.)(sq.ft.)(°F.)
k = thermal conductivity, B.t.u./(hr.)(ft.)(°F.)
K = $(\gamma/\rho g)^{1/2}$, ft.
L = length of plate, ft.
M = molecular weight, lb.$_m$/mole
q = heat flux, B.t.u./(hr.)(sq.ft.)
R = gas constant
T = temperature, °F.
t = saturation temperature, °R.
V = specific volume of vapor cu.ft./lb.$_m$
x = distance from back at plate, ft.
X = meniscus height, ft.
y = distance from back at plate, ft.
Y = distance from base of meniscus, ft.

Greek Letters

γ = liquid surface tension, lb.$_f$/ft.
δ = meniscus thickness, ft.
η = dimensionless y coordinate
θ = dimensionless temperature
λ = latent heat of evaporation, B.t.u./lb.$_m$
σ = evaporation coefficient
ξ = dimensionless χ coordinate
ρ = density, lb.$_m$/cu.ft.
ϕ = contact angle, deg.

Subscripts

B = bottom of plate
c = center line
l = liquid surface
s = solid surface
T = top of plate

LITERATURE CITED

1. Wayner, P. C., Jr., and S. G. Bankoff, *AIChE J.*, **11**, 59 (1965).
2. Pai, V. K., and S. G. Bankoff, *ibid.*, **11**, 65 (1956).
3. Wayner, P. C., Jr. and A. S. Kesten, *ibid.*, **11**, 858 (1965).
4. Bressler, R. G., and P. W. Wyatt, *J. Heat Transfer*, **92c**, 126 (1970).
5. Coccio, C. L., Ph.D. thesis, Rensselaer Polytechnic Inst., Troy, N. Y. (1969).
6. McNutt, J., and G. M. Andes, *J. Chem. Phys.*, **30**, 1300 (1959).
7. Nabavian, K., and L. A. Bromley, *Chem. Eng. Sci.*, **18**, 651 (1963).
8. Nabavian, K., Ph.D. thesis, Univ. California, Berkeley (1962).

Manuscript received October 29, 1969; revision received March 30, 1970; paper accepted April 3, 1970. Paper presented at AIChE Atlanta meeting.